ATMOSPHERIC SCIENCE LETTERS
Atmos. Sci. Let. **17**: 501–509 (2016)
Published online 3 August 2016 in Wiley Online Library
(wileyonlinelibrary.com) **DOI:** 10.1002/asl.684

RMetS
Royal Meteorological Society

An interdecadal shift in the number of hot nights around 1997 over Eastern China

Sisi Chen,[1,2,*] Jingyong Zhang[1] and Gang Huang[3]
[1] *Center for Monsoon System Research, Institute of Atmospheric Physics, Chinese Academy of Sciences, Beijing, China*
[2] *University of Chinese Academy of Sciences, Beijing, China*
[3] *State Key Laboratory of Numerical Modeling for Atmospheric Sciences and Geophysical Fluid Dynamics (LASG), Institute of Atmospheric Physics, Chinese Academy of Sciences, Beijing, China*

**Correspondence to:*
S. Chen, Center for Monsoon System Research, Institute of Atmospheric Physics, Chinese Academy of Sciences, Beijing 100029, China.
E-mail: css@mail.iap.ac.cn

Received: 12 November 2015
Revised: 5 July 2016
Accepted: 12 July 2016

Abstract

In this study, we investigate the interdecadal variation in summer nighttime hot extremes over eastern China using observational daily minimum temperature during 1979–2013. Results show a statistically significant shift in the number of hot nights (NHN) around 1997 with averaged NHN over eastern China of 6 days more during 1997–2013 than 1979–1996. The time series of the first leading Empirical Orthogonal Function mode of the NHN is closely related with sea surface temperature anomalies over the tropical western pacific warm pool, Pacific Decadal Oscillation and Atlantic Multidecadal Oscillation, which all experienced substantial interdecadal changes in the late 1990s. Other factors such as the Urban Heat Island (UHI) effects may also contribute to the interdecadal change of the NHN around 1997.

Keywords: **temperature extreme; nighttime; eastern China; interdecadal variation**

1. Introduction

High-temperature extremes have much more substantial effects on human lives and property than mean temperature (e.g. Meehl and Tebaldi, 2004; Fischer *et al.*, 2007; Seneviratne *et al.*, 2014). This was evident in several recent heat waves, which generally refer to three or more consecutive hot days, including the devastating summer of 2003, with 66 000 deaths in Europe (e.g. Luterbacher *et al.*, 2004), the disastrous high-temperature extreme that struck the Russian Federation in 2010, causing over 55 000 deaths (e.g. Matsueda, 2011), and the record-breaking heat wave that swept the China entirely in 2013, resulting in 59 billion Yuan losses (e.g. Xia *et al.*, 2016). Observational data shows that heat extremes continue to increase over land, even during the so-called global warming hiatus period of 1998–2012 (e.g. Seneviratne *et al.*, 2014).

In China, the mean temperature has been increasing, especially after the 1980s (e.g. Li *et al.*, 2012). Temperature extremes become more likely to occur frequently with the increase in mean temperature (e.g. Gong *et al.*, 2004; Ren *et al.*, 2010a; You *et al.*, 2011; Xia *et al.*, 2016). China has not only experienced significant increase in hot days, but also witnessed an increase in the frequency of hot nights in recent decades (e.g. Cao *et al.*, 2013; Ren and Zhou, 2014; Sun *et al.*, 2014). Ding *et al.* (2010) demonstrated that extreme hot days have increased significantly in most of China, with a rising rate of 4 days per decade over the northern China between 1961 and 2007. Hot days exhibited a notable increase after the late 1990s in China (e.g. Wei and Chen, 2011; Li *et al.*, 2012). Zhou and Ren (2011) found that warm nights increased at a rate of 8.16 days/10 years, which is faster than that of warm days (5.22 days/10 years) in China between 1961 and 2008.

Previous studies focus mainly on the climatology, interannual variability and trends of high-temperature extremes, particularly on daytime hot extremes in China (e.g. Qian *et al.*, 2007; Ren *et al.*, 2010a; Qian *et al.*, 2011; Yan *et al.*, 2011; Zhang and Wu, 2011; Cao *et al.*, 2013; Huang *et al.*, 2014a; Ren and Zhou, 2014). A few studies have analyzed the interdecadal variations of daytime hot extremes (e.g. Wei and Chen, 2011; Li *et al.*, 2012). Less attention, however, has been devoted to the interdecadal variations of hot extremes at night. In this study, we investigate the interdecadal variation of summer nighttime hot extremes over eastern China, which is the most populated and developed area of China, and further discuss possible physical mechanisms involved.

2. Data and methods

In this study, we use updated homogenized daily minimum temperature data from the China Homogenized Temperature dataset based on Multiple Analysis of Series for Homogenization (MASH), namely CHTM 3.0 between 1960 to 2013, at 753 national reference meteorological stations in China (e.g. Li *et al.*, 2016). The CHTM 3.0 data was produced using the MASH method to detect and adjust inhomogeneities and using the technique proposed by Li *et al.* (2015) to maintain physical consistency in temperature series. It has been

© 2016 The Authors. *Atmospheric Science Letters* published by John Wiley & Sons Ltd on behalf of the Royal Meteorological Society.
This is an open access article under the terms of the Creative Commons Attribution License, which permits use, distribution and reproduction in any medium, provided the original work is properly cited.

suggested that CHTM 3.0 is more reasonable and suitable for large-scale climate change analyses in China compared to other datasets (e.g. Li *et al.*, 2016). Previous studies have indicated an abrupt climatic shift around 1980 (e.g. Ding *et al.*, 2008, Tu *et al.*, 2010). In this study, we focus on the period of 1979–2013, after this climatic shift. Nighttime hot extremes were estimated using the number of hot nights (NHN) in summer (June–July–August, JJA) at 431 stations in the east of 110°E in China (Figure 1). Following previous studies, the NHN index was defined as the number of days at each station where the daily minimum temperature meets or exceeds the long-term mean 90th percentile of daily minimum temperature (e.g. Fischer *et al.*, 2007; Zhang and Wu, 2011). For each of the 35 years analyzed between 1979 and 2013, the 90th percentile was based on the 92-day JJA period. The long-term mean 90th percentile was calculated as the mean of the 90th percentile daily minimum temperatures over these 35 years. Similar conclusions were obtained using the thresholds of the 95th and 99th percentiles for the NHN, therefore not presented. The sea surface temperature (SST) data was acquired from the National Oceanic and Atmospheric Administration (NOAA) Extended Reconstructed SST (ERSST v4; e.g. Huang *et al.*, 2014b) from 1979 to 2013. The Atlantic Multidecadal Oscillation (AMO) index is derived from http://www.esrl.noaa.gov/psd/data/timeseries/AMO/ for the period of 1979–2013, while the Pacific Decadal Oscillation (PDO) index for the same period is obtained from http://research.jisao.washington.edu/pdo/. The geopotential height and total column water vapor data are acquired from the European Center Medium-Range Weather Forecasts (ECMWF) ERA-Interim reanalysis datasets (e.g. Berrisford *et al.*, 2011) from http://apps.ecmwf.int/datasets/data/interim-full-daily/levtype=sfc/ for the period covering 1979–2013.

Empirical Orthogonal Function (EOF) analysis (e.g. Lorenz, 1956) was used to obtain the first dominant mode of the NHN and associated time series over eastern China during 1979–2013. The EOF analysis was performed based on the covariance matrix of normalized departures of NHN. The fast Fourier transform (FFT) method was used to separate the relevant time series of the NHN and SST on different scales. The Mann–Kendall (MK) technique (e.g. Mann, 1945; Kendall, 1975) was used to test the abrupt change point of the trend (see Appendix). According to the theory of the MK's test, when the value of statistic UF is positive, it indicates that the factor being tested has an increasing trend. In contrast, a negative value indicates a decreasing trend. Furthermore, the trend passes the 95% confidence level when the value of UF is greater (lower) than 1.96 (−1.96).

3. Results

Figure 2 shows the spatial variation of the first leading EOF mode (EOF1, Figure 2(a)) and the climate mean

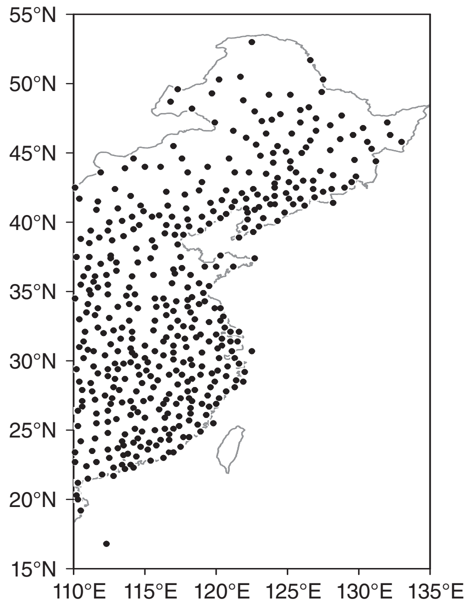

Figure 1. Geographic distribution of 431 meteorological stations in the east of 110°E of China.

state (Figure 2(b)) of summer NHN over eastern China between 1979 and 2013. EOF1 accounts for 40% of the variance and can be well separated from the lower modes based on the criterion defined by North *et al.* (1982). The spatial distribution of EOF1 (Figure 2(a)) is featured by same-sign anomalies of the NHN over eastern China, indicating that nighttime hot extremes change consistently over all of the eastern China over 1979–2013. Hence, the EOF1 of the NHN is the sole mode discussed in our examination of the variation of the NHN. The largest values of EOF1 occur around the middle part of eastern China, while weaker values are found in the southern part of the region (Figure 2(a)). This indicates that nighttime hot extremes occurred more in the middle than other parts of eastern China. The spatial distribution of the climate mean state of the NHN shows that NHN also occurred more around the middle part of eastern China between 1979 and 2013 (Figure 2(b)), which overall coincides with the spatial pattern of EOF1. Besides, high occurrence areas where the occurrence of the NHN exceeds 10.5 days are also scattered across the North China.

Figure 3(a) displays temporal features of the time series associated with EOF1 and annual area mean days of the NHN over eastern China over 1979–2013. According to Figure 1, the 431 meteorological stations are spread almost evenly in eastern China. Thus the annual area mean days of NHN is computed from annual summer NHN averaged over the 431 stations as the general occurrence state of summer NHN in eastern China for each year. The long-term mean NHN is 10.6 days per year in summer over the period of 1979–2013. Changes in the two time series are consistent with each other, and the correlation coefficient between them reaches a significance of 0.99 at the 99% confidence level (Figure 3(a)). Both time series of EOF1 and annual area mean NHN show significant

© 2016 The Authors. *Atmospheric Science Letters* published by John Wiley & Sons Ltd on behalf of the Royal Meteorological Society.

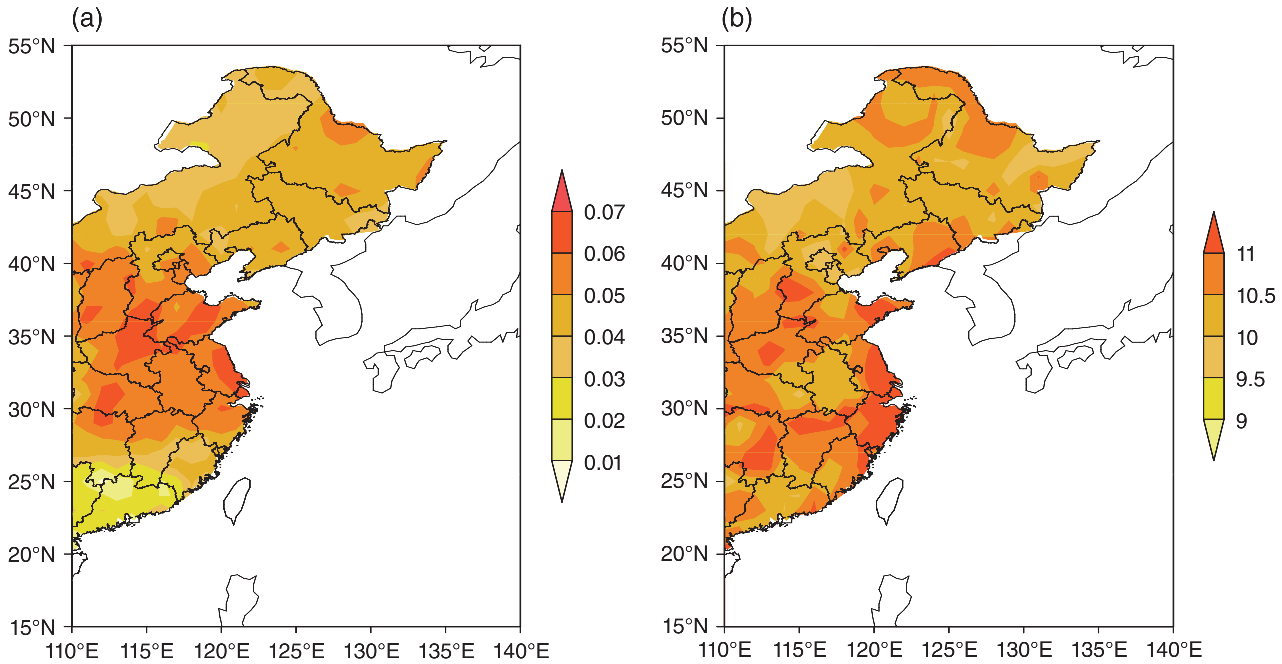

Figure 2. Spatial distribution of (a) the EOF1 (the first leading Empirical Orthogonal Function) and (b) the climate mean state (in days) of summer (June–July–August, JJA) NHN (number of hot nights) over eastern China over the period 1979–2013.

increasing trends. The interannual and interdecadal variations are obvious in both time series. The time series of EOF1 are further separated into interannual and interdecadal scales using the FFT (Figure 3(b)). There are distinct interannual and interdecadal variations in EOF1, with clear increasing interdecadal trend. It is worth noting that the interdecadal variation of the time series of EOF1 enhanced abruptly around the late 1990s. Figure 3(a) and (b) show that eastern China experienced a rise in summer NHN during the period of 1979–2013, and a sudden jump in summer NHN may have occurred in the late 1990s. To confirm this abrupt increase, we further analyze the time series of EOF1 and annual area mean NHN using the MK technique, as showed in Figure 3(c) and (d), respectively. Both time series reflect abrupt increases in 1997. The average NHN before and after 1997 is approximately 7.7 and 13.7 days, respectively (Figure 3(a)). According to the UF values in Figure 3(c) and (d), the NHN increased from the early 1990s, and rose significantly (statistically significant at the 95% confidence level; ± 1.96) after 1999. Figure 3 shows that summer nighttime hot extremes increased over eastern China over the period of 1979–2013, and a climatic abrupt phenomenon of interdecadal increase occurred in 1997. The average number of nighttime hot extremes increased by 6 days after 1997 over eastern China.

To better understand the interdecadal variation in 1997, differences of NHN between 1997–2013 and 1979–1996 over eastern China are shown in Figure 4. The differences represent the changes in summer nighttime hot extremes after 1997 over eastern China. Compared to the period between 1979 and 1996, NHN in most regions of eastern China have increased by more than 5 days between 1997 and 2013. This interdecadal increase of nighttime hot extremes after 1997 is in accordance with daytime hot extremes researched in previous study (e.g. Li *et al.*, 2012).

4. Discussion of possible physical mechanisms

SST anomalies may be one possible cause for the interdecadal increase of the NHN after 1997 by influencing atmospheric circulation and climate anomalies (e.g. Xie *et al.*, 2009; Li *et al.*, 2010; Wu *et al.*, 2010; Hu *et al.*, 2011; Huang *et al.*, 2011). SST anomalies can affect atmospheric circulation via the air–sea interactions including convective activities and surface energy fluxes (e.g. Xie *et al.*, 2009; Hu *et al.*, 2013). Air–sea interactions force the atmosphere to adjust itself through developing anomalous anticyclone or cyclone. Anomalous anticyclones or cyclones subsequently influence surface air temperature by changing the temperature advection, vertical motion and adiabatic heating (e.g. Hu *et al.*, 2011).

Figure 5(a) shows the spatial pattern of correlation coefficients of the EOF1 time series of summer NHN with simultaneous SST. The strongest relationship can be seen observed in the Tropical Western Pacific Warm Pool (TWPWP) region (0–20°N, 130–160°E). The correlation coefficient between summer mean SST averaged over the TWPWP region and the EOF1's time series is 0.74 which is statistically significant at the 99% confidence level. There is an increasing trend in the time series of SST (Figure 5(b)). The interannual and interdecadal variations, which are separated by using FFT, of the summer mean SST averaged over the TWPWP region are significant in Figure 5(c). A rise in

© 2016 The Authors. *Atmospheric Science Letters* published by John Wiley & Sons Ltd on behalf of the Royal Meteorological Society.

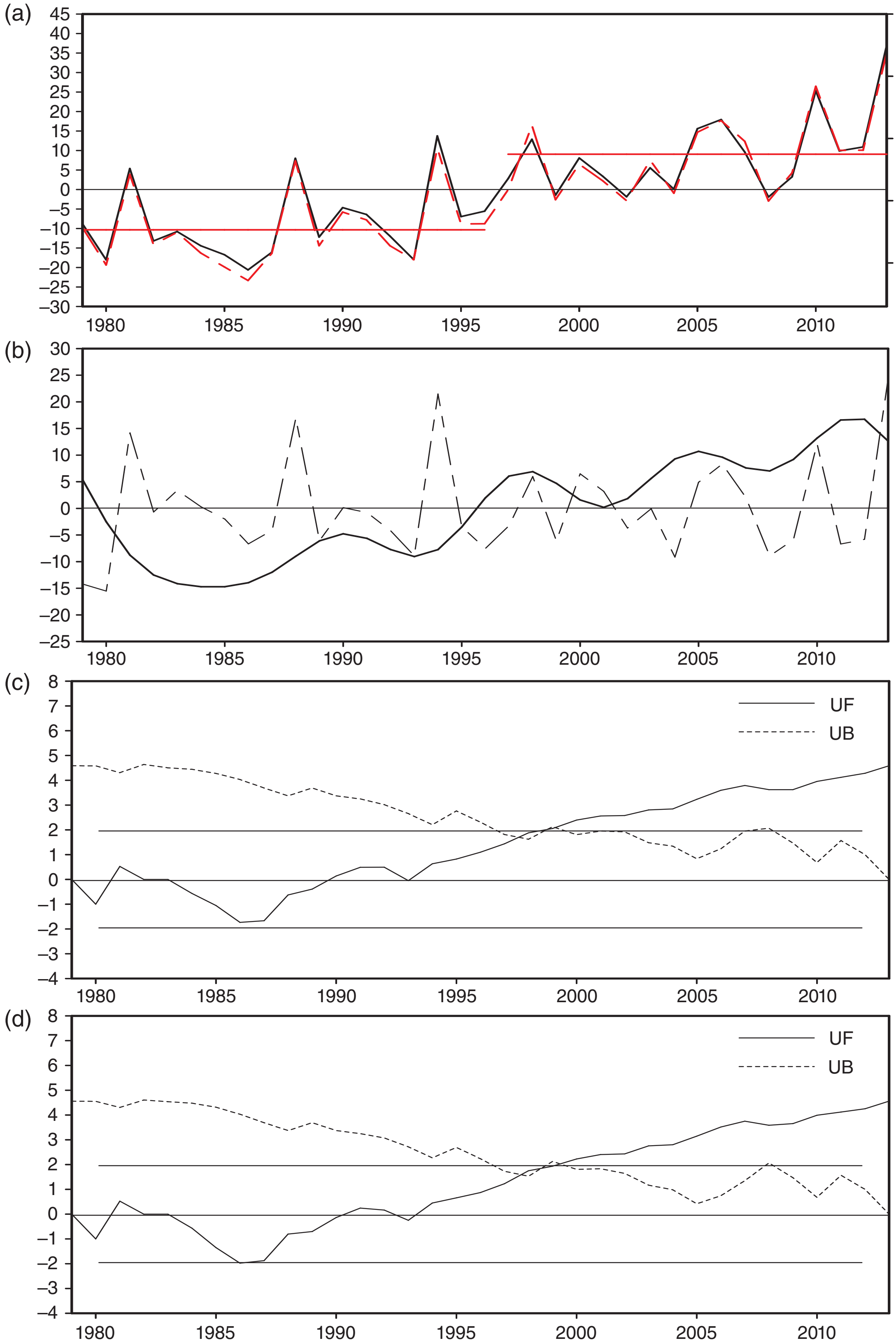

Figure 3. (a) Time series of the EOF1 (solid curve, left ordinate) and annual area mean NHN (dashed red curve, right axis, in days) over eastern China between 1979 and 2013. The black horizontal line refers to 0 on the left axis for the time series ofEOF1 and to the long-term mean NHN on the right axis for the time series of annual area mean NHN. The solid red lines are corresponding to averaged days of annual area mean NHN over 1979–1996 and 1997–2013 periods, respectively. (b) Interannual (dashed curve) and interdecadal (solid curve) variations of the time series of EOF1 separated by fast Fourier transform method (FFT). (c) Mann–Kendall test (MK) for the time series of EOF 1 and (d) annual area mean NHN (The solid horizontal line is the 95 % confidence level (±1.96) according to the Student's *t*-test.).

© 2016 The Authors. *Atmospheric Science Letters* published by John Wiley & Sons Ltd on behalf of the Royal Meteorological Society.

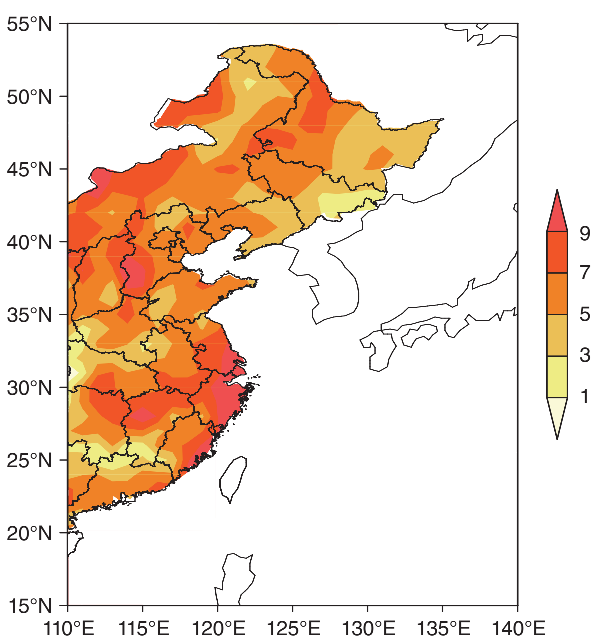

Figure 4. Composite differences of NHN (in days) between the periods of 1979–1996 and 1997–2013 (1997–2013 minus 1979–1996) over eastern China.

the SST is observed around the mid-1990s, both in the time series (Figure 5(b)) and interdecadal variations (Figure 5(c)).The MK test of the SST (not shown) indicates that an abrupt increase of SST occurs in 1994 and significant increases start from 1997. Summer mean SST averaged over the TWPWP between 1979 and 1996 is about 29.3 °C, while it rises up to 29.6 °C between 1997 and 2013 (Figure 5(b)). Considering the high correlation between EOF1's time series of the NHN and summer mean SST averaged over the TWPWP, the interdecadal increase of the SST around the mid-1990s may represent an important contribution to the interdecadal increase of the NHN over eastern China.

Previous studies have demonstrated that the SST anomaly in the TWPWP has significant impacts on summer climate over East Asia (e.g. Huang and Sun, 1994b; Huang and Sun, 1994a; Zhao *et al.*, 2002; Zhao *et al.*, 2002; Huang *et al.*, 2006; Zhang *et al.*, 2006). When the SST gets warmer around the TWPWP, the western Pacific subtropical high (WPSH) shifts northward, extends westward and intensifies by the propagation of quasi-stationary planetary waves caused by accelerated convection and the enhancement of a Hadley cell (e.g. Huang and Li, 1988; Huang and Lu, 1989; Huang and Sun, 1994b; Huang and Sun, 1994a; Zhao *et al.*, 2002; Zhang *et al.*, 2006). The interdecadal increase of SST in the TWPWP tends to intensify the WPSH and increase the geopotential height at 500 hPa (Figure 6(a)), and subsequently rise up the daytime surface air temperature through increasing surface solar radiation absorption and enhancing subsidence warming (e.g. Zhang *et al.*, 2005; Baldi *et al.*, 2006; Lei *et al.*, 2009; Wei and Chen, 2011). With daytime temperature rising, the temperature persistence between day and night will contribute to the nighttime high temperature which favors nighttime hot extremes (e.g. Chen and Lu, 2014). The SST anomaly in the TWPWP is closely associated with the atmospheric water vapor in East Asia by influencing the Asian summer monsoon and atmospheric circulation (e.g. Huang and Sun, 1994b; Huang *et al.*, 2006; Zhang *et al.*, 2006; Xiang and Wang, 2013). Previous studies show that positive SST anomalies in the TWPWP intensify local convective activities and create a very strong anticyclone circulation in the lower troposphere over the western Pacific Ocean (e.g. Huang and Sun, 1994b; Huang and Sun, 1994a; Jin and Chen, 2002), which strengthen the Asian summer monsoon (e.g. Jin and Chen, 2002). Thus, more water vapor can be transported by the strong Asian summer monsoon flow from the TWPWP into eastern China (e.g. Huang and Chen, 2010). Figure 6(b) shows that the interdecadal increase of SST in the TWPWP tends to increase the nighttime total column water vapor over North China and some other areas of eastern China. The increased atmospheric water vapor condition can result in more downward longwave radiation and warm up the nighttime surface air temperature, favoring the occurrence of nighttime hot extremes (e.g. Wei and Sun, 2007; Gershunov *et al.*, 2009; Ha and Yun, 2012; Chen and Lu, 2014; Lu and Chen, 2016).

Other factors such as the large-scale patterns and anthropogenic forcing may be contributing to the abrupt increase of summer NHN over eastern China. The Atlantic Multidecadal Oscillation (AMO) and the Pacific Decadal Oscillation (PDO) are large-scale patterns in regulating decadal changes of surface air temperature (e.g. Knight *et al.*, 2006; Deser *et al.*, 2010) for many regions such as East Asia (e.g. Zhu and Yang, 2003; Gao *et al.*, 2015; Xia *et al.*, 2016). Correlation coefficients between EOF1's time series of NHN and the AMO and PDO indices are 0.58 and −0.46 (both statistically significant at the 99% confidence level), respectively, for the 1979–2013 period, indicating that AMO and PDO are closely related to NHN over eastern China. In Figure 7, interdecadal variations around the late 1990s are seen in both the AMO and the PDO time series. The long-term mean AMO (PDO) index is about −0.06 (0.8) over 1979–1996 and it changes to be about 0.2 (−0.2) over 1997–2013 (Figure 7). There are substantial interdecadal differences in AMO and PDO between 1997 and 2013 compared to these observed between 1979 and 1996. The changes in AMO and PDO are conducive of the interdecadal increase of NHN after 1997.

The impacts of anthropogenic forcing such as the Urban Heat Island (UHI) effects on nighttime hot extremes in China also cannot be ignored (e.g. Zhou and Ren, 2009; Ren *et al.*, 2010b; Wu and Yang, 2013; Ren and Zhou, 2014; Zhou *et al.*, 2014). Ren and Zhou (2014) indicated that the increasing trend of nighttime hot extremes in summer contributed to by UHI reaching up to 3.435 days (10 years)$^{-1}$, which accounts for 33.7% of the overall increase in mainland China between 1961 and 2008. The UHI-induced increase of nighttime hot

© 2016 The Authors. *Atmospheric Science Letters* published by John Wiley & Sons Ltd on behalf of the Royal Meteorological Society.

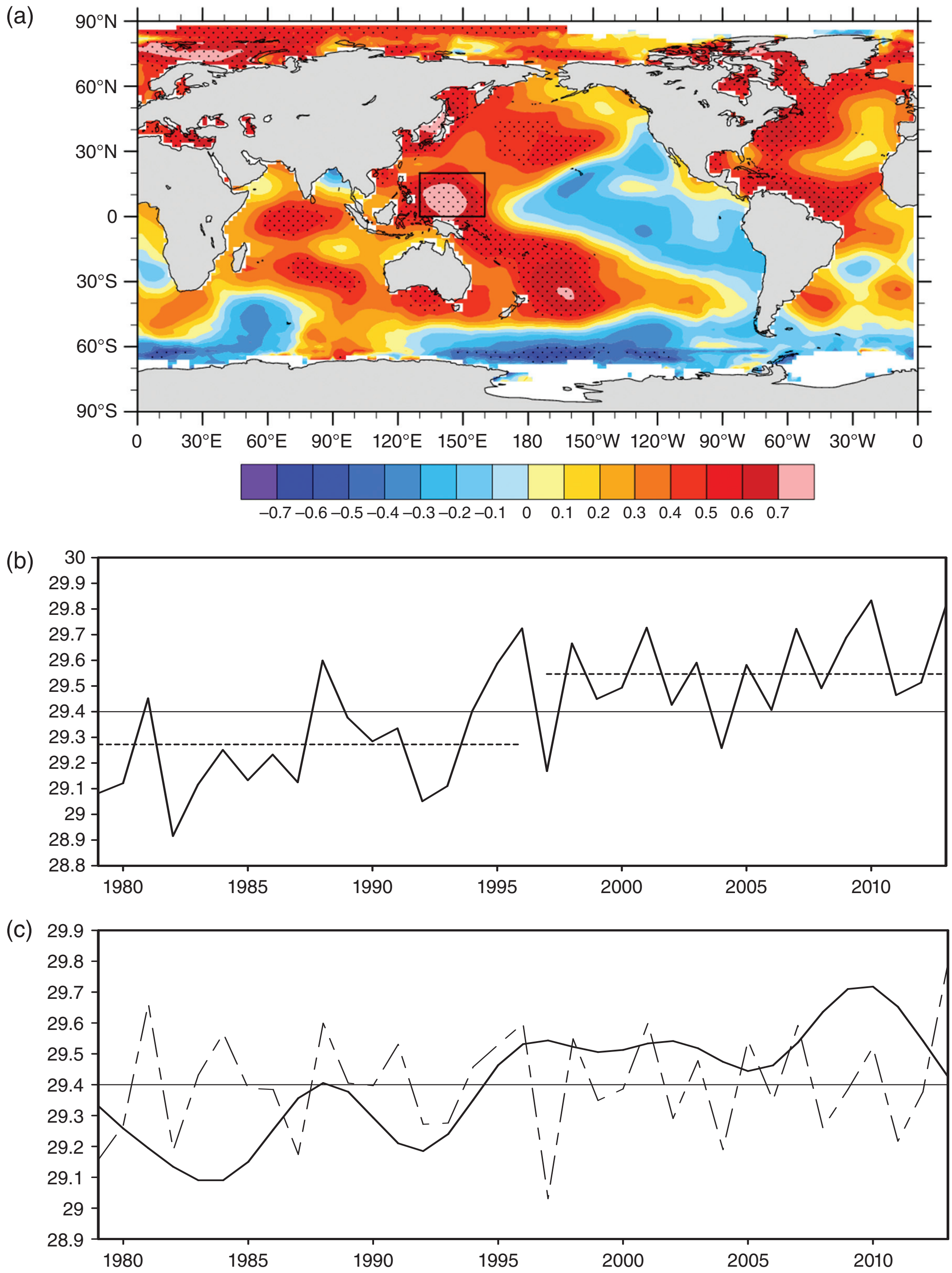

Figure 5. (a) Correlation map of EOF1's time series with reference to simultaneous summer mean Sea Surface Temperature (SST). The dotted regions denote correlation coefficients significant at 99% confidence level. (b) Time series of summer mean SST (in centigrade degrees) averaged over the TWPWP (Tropical West Pacific Warm Pool, 0–20°N, 130–160°E) region marked by a box in (a). The solid horizontal line denotes the long-term mean SST in TWPWP for the 1979–2013 period and short dashed lines for the period of 1979–1996 and 1997–2013, respectively. (c) Interannual (dashed curve) and interdecadal (solid curve) variations of the time series of summer mean SST (in centigrade degrees) averaged over the TWPWP separated by fast Fourier transform method.

extremes dominantly appeared after the beginning of the 1990s. Considering that eastern China is densely populated and hosts many megacities, the UHI effects are favorable to the interdecadal variation of NHN.

It should be kept in mind that physical mechanisms cannot be fully extracted by using statistical analyses. In the future, further studies on the model simulations to test the proposed mechanisms are needed to explain the abrupt interdecadal variation.

5. Conclusions

In this study, we investigate the interdecadal variation of summer nighttime hot extremes for the period of

© 2016 The Authors. *Atmospheric Science Letters* published by John Wiley & Sons Ltd on behalf of the Royal Meteorological Society.

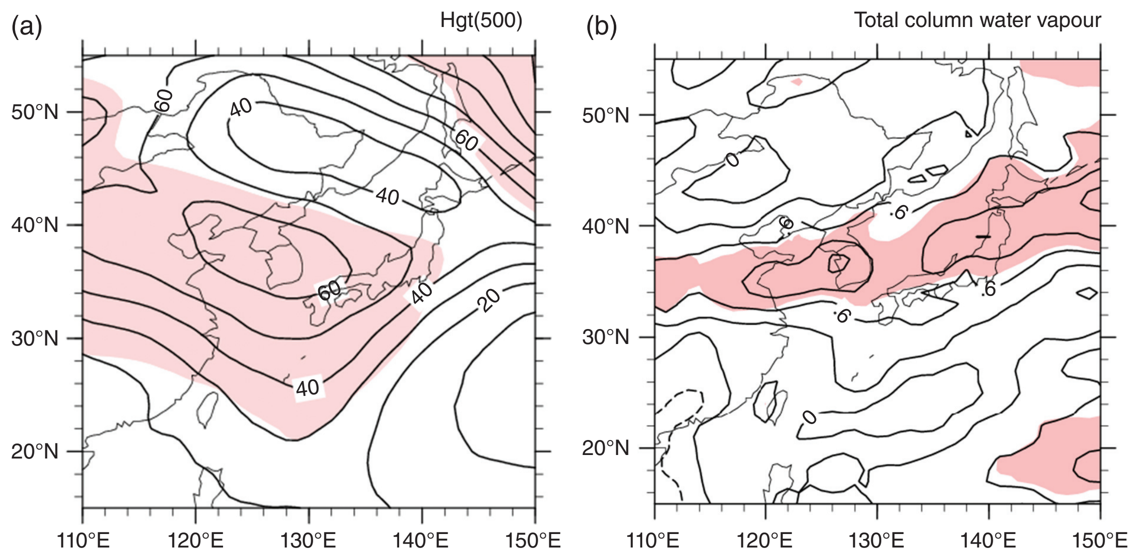

Figure 6. Anomalies of the summer averaged geopotential height in the daytime at 500 hPa (a) with unit $m^2\ s^{-2}$ and total column water vapor in the nighttime (b) with unit kg m^2 in 1979–2013, obtained using regressions on normalized summer mean SST averaged in the TWPWP. The shading indicates the anomalies that are significant at 95 % confidence level.

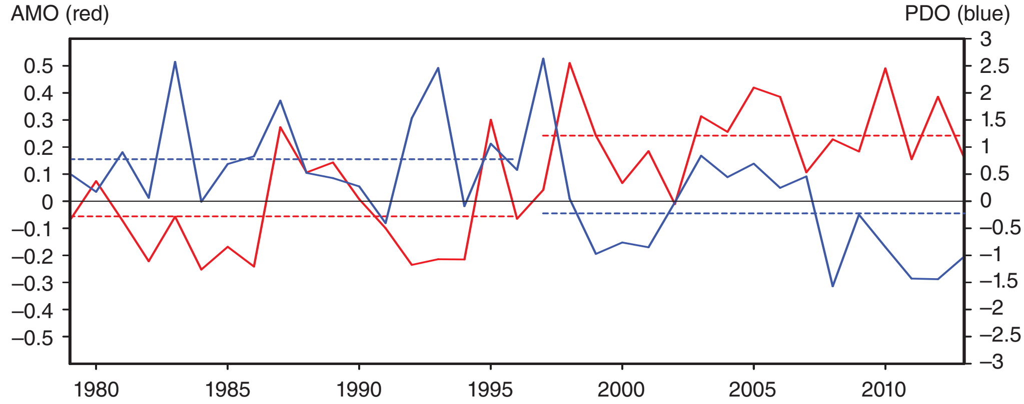

Figure 7. Time series of the summer Atlantic Multidecadal Oscillation (AMO) index in red on the left axis and the Pacific Decadal Oscillation (PDO) index in blue on the right axis between 1979 and 2013.The black solid line refers to 0 for both indices. The short horizontal and dashed red (blue) lines denote long-term mean values of AMO cuPDO) for 1979–1996 and 1997–2013, respectively.

1979–2013 over eastern China. Previous analyses and this study show consistently increasing nighttime hot extremes in recent decades (e.g. Qian *et al.*, 2011; You *et al.*, 2011; Zhou and Ren, 2011). We further identify a statistically significant shift of the number of hot nights (NHN) that occurred around 1997 over eastern China. The averaged NHN over eastern China between 1997 and 2013 was 6 days more than that measured between 1979 and 1996, with most regions having experienced an increase of more than 5 days after 1997. The possible physical mechanisms that may be invoked to explain the interdecadal variation of NHN around 1997 over eastern China are discussed. The time series of the first leading Empirical Orthogonal Function mode of summer NHN is closely related to the simultaneous sea surface temperatures (SST) in the tropical western pacific warm pool (TWPWP) which also experience substantial interdecadal increase around the late-1990s ($r = 0.74$). The interdecadal increase of SST in the TWPWP tend to increase the geopotential height at 500 hPa and the total column water vapor by intensifying the western Pacific subtropical high (WPSH) and influencing the Asian summer monsoons and atmospheric circulation. Increased geopotential heights at daytime and water vapor at nighttime favored the occurrence of nighttime hot extremes after 1997. The interdecadal variation of NHN is also closely associated with the summer Atlantic Multidecadal Oscillation (AMO) and Pacific Decadal Oscillation (PDO) with correlation coefficients of 0.58 and −0.46, respectively. The same shifts are revealed in both the AMO and PDO indices around the late-1990s. The effects of the Urban Heat Island (UHI) on nighttime hot extremes may also contribute to the interdecadal variation of the NHN.

Causes for the abrupt increase of summer NHN, over eastern China, can be mixed and complicated. The proposed physical mechanisms cannot account for the whole of the interdecadal variation around 1997, and other factors such as The Tibetan Plateau (TP) snow and soil moisture may also play roles (e.g. Ding *et al.*, 2009; Zhang and Dong, 2010). These proposed mechanisms explaining the interdecadal variation of the NHN over eastern China need to be further tested and clarified using model simulations in future.

Acknowledgements

This work was supported by the National Basic Research Program of China (2012CB955604) and the National Natural Science Foundation of China (Grant No. 41275089). Jingyong Zhang was also supported by the Jiangsu Collaborative Innovation Center for Climate Change.

Appendix: Mann–Kendall (MK) test

The MK test is based on the statistic S_k defined as follows:

$$S_k = \sum_{i=1}^{k} r_i, \quad k = 2,\ 3,\ \dots,\ n$$

where

$$r_i = \begin{cases} +1, & \text{if } x_i > x_j, \\ 0, & \text{if } x_i < x_j, \end{cases} \quad j = 1,\ 2,\ \dots,\ i$$

and x_i are the sequential values and n is the length of the data set.

The statistic UF is computed by

$$\mathrm{UF}_k = \frac{\left[S_k - E\left(S_k\right)\right]}{\sqrt{\mathrm{var}\left(S_k\right)}}, \ k = 1,\ 2,\ \dots,\ n$$

where $\mathrm{UF}_1 = 0$, the $E(S_k)$ and $\mathrm{var}(S_k)$ are mean and variance of S_k, respectively, which can be computed as follow:

$$\begin{cases} E\left(S_k\right) = \frac{k(k-1)}{4}, \\ \mathrm{var}\left(S_k\right) = \frac{k(k-1)(2k+5)}{72}, \end{cases} \quad k = 2,\ 3,\ \dots,\ n$$

The statistic UF_k follows the standard normal distribution and is calculated from x in the time series of $x_1, x_2, \dots, x_n$.

The other statistic UB used in this paper is computed in a similar manner as UF, from x in reverse order ($x_n, x_{n-1}, \dots, x_1$), and

$$\mathrm{UB}_k = -\mathrm{UF}_k\ (k = n,\ n-1,\ \dots,\ 1),\ \mathrm{UB}_1 = 0$$

References

Baldi M, Dalu G, Maracchi G, Pasqui M, Cesarone F. 2006. Heat waves in the Mediterranean: a local feature or a larger-scale effect? *International Journal of Climatology* **26**: 1477–1487.

Berrisford P, Dee D, Poli P, Brugge R, Fielding K, Fuentes M, Kallberg P, Kobayashi S, Uppala S, Simmons A. 2011. The ERA-Interim Archive Version 2.0. ERA Report Series **1**:1–16.

Cao L, Zhao P, Yan Z, Jones P, Zhu, Yu Y, Tang G. 2013. Instrumental temperature series in eastern and central China back to the nineteenth century. *Journal of Geophysical Research, [Atmospheres]* **118**: 8197–8207.

Chen R, Lu R. 2014. Dry tropical nights and wet extreme heat in Beijing: atypical configurations between high temperature and humidity. *Monthly Weather Review* **142**: 1792–1802.

Deser C, Alexander MA, Xie S, Phillips AS. 2010. Sea surface temperature variability: Patterns and mechanisms. *Marine Science* **2**: 115–143.

Ding Y, Wang Z, Ying S. 2008. Interdecadal variation of the summer precipitation in East China and its association with decreasing Asian summer monsoon. Part I: Observed evidences. *International Journal of Climatology* **28**: 1139–1162.

Ding Y, Sun Y, Wang Z, Zhu Y, Song Y. 2009. Interdecadal variation of the summer precipitation in China and its association with decreasing Asian summer monsoon Part II: possible causes. *International Journal of Climatology* **29**: 1926–1944.

Ding T, Qian W, Yan Z. 2010. Changes in hot days and heat waves in China during 1961–2007. *International Journal of Climatology* **30**: 1452–1462.

Fischer EM, Seneviratne SI, Lüthi D, Schär C. 2007. Contribution of land-atmosphere coupling to recent European summer heat waves. *Geophysical Research Letters* **34**: 6.

Gao L, Yan Z, Quan X. 2015. Observed and SST-forced multidecadal variability in global land surface air temperature. *Climate Dynamics* **44**: 359–369.

Gershunov A, Cayan D, Iacobellis S. 2009. The great 2006 heat wave over California and Nevada: signal of an increasing trend. *Journal of Climate* **22**: 6181–6203.

Gong D, Pan Y, Wang J. 2004. Changes in extreme daily mean temperatures in summer in eastern China during 1955–2000. *Theoretical and Applied Climatology* **77**: 25–37.

Ha K, Yun K. 2012. Climate change effects on tropical night days in Seoul, Korea. *Theoretical and Applied Climatology* **109**: 191–203.

Hu K, Huang G, Huang R. 2011. The impact of tropical Indian Ocean variability on summer surface air temperature in China. *Journal of Climate* **24**: 5365–5377.

Hu K, Huang G, Wu R. 2013. A strengthened influence of ENSO on August high temperature extremes over the Southern Yangtze River Valley since the Late 1980s. *Journal of Climate* **26**: 2205–2221.

Huang R, Chen J. 2010. Characteristics of the summertime water vapor transports over the eastern part of China and those over the western part of China and their difference. *Chinese Journal of Atmospheric Sciences* **34**: 1035–1045.

Huang R, Li W. 1988. Influence of heat source anomaly over the western tropical Pacific on the subtropical high over East Asia and its physical mechanism. *Scientia Atmospherica Sinica (Special Issue)* **12**: 95–107.

Huang R, Lu L. 1989. Numerical simulation of the relationship between the anomaly of subtropical high over East Asia and the convective activities in the western tropical Pacific. *Advances in Atmospheric Sciences* **6**: 202–214.

Huang R, Sun F. 1994a. Impacts of the thermal state and the convective activities in the tropical western warm pool on the summer climate anomalies in east Asia. *Chinese Journal of Atmospheric Sciences* **2**: 001.

Huang R, Sun F. 1994b. Impact of the convective activities over the western tropical pacific warm pool on the intraseasonal variability of the east Asian summer monsoon. *Chinese Journal of Atmospheric Sciences* **4**: 009.

Huang R, Gu L, Zhou L, Wu S. 2006. Impact of the thermal state of the tropical western Pacific on onset date and process of the South China Sea summer monsoon. *Advances in Atmospheric Sciences* **23**: 909–924.

Huang G, Qu X, Hu K. 2011. The impact of the tropical Indian Ocean on South Asian high in boreal summer. *Advances in Atmospheric Sciences* **28**: 421–432.

Huang F, Hu B, Zhou X, Fang Y. 2014a. Multi-scale variations of winter extreme minimum temperature in China (in Chinese). *Periodical of Ocean University of China* **40**: 042–050.

Huang B, Banzon VF, Freeman E, Lawrimore J, Liu W, Peterson TC, Smith TM, Thome PW, Woodruff SD, Zhang H. 2014b. Extended reconstructed sea surface temperature version 4 (ERSST.v4): part I. upgrades and intercomparisions. *Journal of Climate* **28**: 911–930.

© 2016 The Authors. *Atmospheric Science Letters* published by John Wiley & Sons Ltd on behalf of the Royal Meteorological Society.

Jin Z, Chen J. 2002. A composite study of the influence of SST warm anomalies over the western Pacific warm pool on Asian summer monsoon. *Chinese Journal of Atmospheric Sciences* **1**: 005.

Kendall MG. 1975. *Rank Correlation Methods*. Oxford University Press: New York, NY.

Knight JR, Folland CK, Scaife AA. 2006. Climate impacts of the Atlantic multidecadal oscillation. *Geophysical Research Letters* **33**: 17.

Lei Y, Gong D, Zhang Z, Guo D, He X. 2009. Spatial-temporal characteristics of high-temperature events in summer in eastern China and the associated atmospheric circulation. *Geographical Research* **3**: 009.

Li F, Li J, Guan Z. 2010. Interdecadal variations of summer temperature in Northeast China and relationships with Pacific SSTA. *Journal of Meteorology and Environment* **26**: 19–26.

Li J, Dong W, Yan Z. 2012. Changes of climate extremes of temperature and precipitation in summer in eastern China associated with changes in atmospheric circulation in East Asia during 1960–2008. *Chinese Science Bulletin* **57**: 1856–1861.

Li Z, Yan Z, Wu H. 2015. Updated homogenized Chinese temperature series with physical consistency. *Atmospheric and Oceanic Science Letters* **8**: 17–22.

Li Z, Cao L, Zhu Y, Yan Z. 2016. Comparing two homogenized datasets of daily maximum/ mean/minimum temperature series for China during 1960–2013. *Journal of Meteorological Research* **30**: 53–66.

Lorenz EN. 1956. Empirical orthogonal functions and statistical weather prediction. In *Scientific Report No.1: Statistical Forecasting Project*. Massachusetts Institute of Technology Department of Meteorology: Cambridge.

Lu R, Chen R. 2016. A review of recent studies on extreme heat in China. *Atmospheric and Oceanic Science Letters* **9**: 114–121.

Luterbacher J, Dietrich D, Xoplaki E, Grosjean M, Wanner H. 2004. European seasonal and annual temperature variability, trends, and extremes since 1500. *Science* **303**: 1499–1503.

Mann HB. 1945. Nonparametric tests against trend. *Econometrica* **13**: 245–259.

Matsueda M. 2011. Predictability of Euro-Russian blocking in summer of 2010. *Geophysical Research Letters* **38**: L06801, doi: 10.1029/2010GL046557.

Meehl GA, Tebaldi C. 2004. More intense, more frequent, and longer lasting heat waves in the 21st century. *Science* **305**: 994–997.

North GR, Bell TL, Cahalan RF, Moeng FJ. 1982. Sampling errors in the estimation of empirical orthogonal functions. *Monthly Weather Review* **110**: 699–706.

Qian W, Fu J, Zhang W, LIN X. 2007. Changes in mean climate and extreme cliamte in China during the last 40 years. *Advances in Earth Science* **7**: 006.

Qian C, Yan Z, Wu Z, Fu Z, Tu K. 2011. Trends in temperature extremes in association with weather-intraseasonal fluctuations in eastern China. *Advances in Atmospheric Sciences* **28**: 297–309.

Ren G, Zhou Y. 2014. Urbanization effect on trends of extreme temperature indices of national stations over Mainland China, 1961–2008. *Journal of Climate* **27**: 2340–2360.

Ren G, Feng G, Yan Z. 2010a. Progresses in observation studies of climate extremes and changes in Mainland China. *Climatic Environmental Research* **15**: 337–353.

Ren Y, Ren G, Zhang A. 2010b. An overview of researches of urbanization effect on land surface air temperature trends (In Chinese). *Progress in Geography* **29**: 1301–1310.

Seneviratne SI, Donat MG, Mueller B, Alexander LV. 2014. No pause in the increase of hot temperature extremes. *Nature Climate Change* **4**: 161–163.

Sun Y, Zhang X, Zwiers FW, Song L, Wang H, Hu T, Hong Y, Ren G. 2014. Rapid increase in the risk of extreme summer heat in Eastern China. *Nature Climate Change* **4**: 1082–1085.

Tu K, Yan Z, Dong W. 2010. Climatic jumps in precipitation and extremes in drying North China during 1954–2006. *Journal of the Meteorological Society of Japan* **88**: 29–42.

Wei K, Chen W. 2011. An abrupt increase in the summer high temperature extreme days across China in the mid-1990s. *Advances in Atmospheric Sciences* **28**: 1023–1029.

Wei J, Sun J. 2007. The analysis of summer heat wave and sultry weather in North China. *Climatic and Environmental Research* **12**: 453–463.

Wu K, Yang X. 2013. Urbanization and heterogeneous surface warming in eastern China. *Chinese Science Bulletin* **58**: 1363–1373.

Wu R, Yang S, Liu S, Sun L, Lian Y, Gao Z. 2010. Changes in the relationship between Northeast China summer temperature and ENSO. *Journal of Geophysical Research: Atmospheres* **115**: D21107, doi: 10.1029/2010JD014422.

Xia J, Tu K, Yan Z, Qi Y. 2016. The super-heat wave in eastern China during July–August 2013: a perspective of climate change. *International Journal of Climatology* **36**: 1291–1298.

Xiang B, Wang B. 2013. Mechanisms for the advanced Asian summer monsoon onset since the mid-to-late 1990s*. *Journal of Climate* **26**: 1993–2009.

Xie S, Hu K, Hafner J, Tokinaga H, Du Y, Huang G, Sampe T. 2009. Indian Ocean capacitor effect on Indo-western Pacific climate during the summer following El Niño. *Journal of Climate* **22**: 730–747.

Yan Z, Xia J, Qian C, Zhou W. 2011. Changes in seasonal cycle and extremes in China during the period 1960–2008. *Advances in Atmospheric Sciences* **28**: 269–283.

You Q, Kang S, Aguilar E, Pepin N, Flügel WA, Yan Y, Xu Y, Zhang Y, Huang J. 2011. Changes in daily climate extremes in China and their connection to the large scale atmospheric circulation during 1961–2003. *Climate Dynamics* **36**: 2399–2417.

Zhang J, Dong W. 2010. Soil moisture influence on summertime surface air temperature over East Asia. *Theoretical and Applied Climatology* **100**: 221–226.

Zhang J, Wu L. 2011. Land-atmosphere coupling amplifies hot extremes over China. *Chinese Science Bulletin* **56**: 3328–3332.

Zhang M, Fu G, Guo J. 2005. Diagnostical analysis of an extreme high-temperature weather event in North China on 15 July, 2002. *Journal of Ocean University of China* **35**: 183–188.

Zhang L, Xu J, He J. 2006. Recent advances in the western Pacific warm pool studies. *Advances in Marine Science* **24**: 108.

Zhao Y, Wu A, Chen Y, Hu D. 2002. The climatic jump of the western Pacific warm pool and its climatic effects. *Journal of Tropical Meteorology* **4**: 003.

Zhou Y, Ren G. 2009. The effect of urbanization on maximum, minimum temperatures and daily temperature range in North China. *Plateau Meteorology* **28**: 1158–1166.

Zhou Y, Ren G. 2011. Change in extreme temperature events frequency over mainland China during 1961–2008. *Climate Research* **50**: 125.

Zhou T, Ma S, Zou L. 2014. Understanding a hot summer in central eastern China: summer 2013 in context of multimodel trend analysis. *Bulletin of the American Meteorological Society* **95**: S54.

Zhu Y, Yang X. 2003. Relationships between Pacific Decadal Oscillation (PDO) and climate variabilities in China(in Chinese). *Acta Meteorologica Sinica* **61**: 641–654.

© 2016 The Authors. *Atmospheric Science Letters* published by John Wiley & Sons Ltd on behalf of the Royal Meteorological Society.